Post-Liquefaction Free-Field Ground Settlement Case Histories

Franklin R. Olaya, *Ph.D. Candidate, Depart. of Civil and Environmental Eng., Univ. of California, Berkeley, 441 Davis Hall, Univ. of California, Berkeley, CA 94720-1710, U.S.A.; email: folaya@berkeley.edu*
Jonathan D. Bray, *Professor, Depart. of Civil and Environmental Eng., Univ. of California, Berkeley, 453 Davis Hall, Univ. of California, Berkeley, CA 94720-1710, U.S.A.; email: jonbray@berkeley.edu*

ABSTRACT: *Liquefaction-induced ground settlement is a complex process resulting from the combined effects of particle sedimentation and soil reconsolidation due to post-shaking dissipation of excess pore-water pressure. Current empirical models are based on a limited number of field case histories. Consequently, it is difficult to quantify uncertainty in the estimate of post-liquefaction settlement. A database of 205 well-documented ground settlement case histories has been created with the goal to support the development of improved liquefaction-induced ground settlement procedures. This study takes advantage of the numerous site investigations and ground motion recordings following the 2010-2011 Canterbury earthquake sequence and the 2013-2016 northern South Island New Zealand earthquakes. The general geotechnical characteristics of the sites are described, and the procedures used to process the CPT data and the models used to estimate ground motion intensity measures are summarized. The survey techniques employed to estimate liquefaction-induced ground settlement are discussed. The characteristics of a well-defined post-liquefaction ground settlement field case history is shared to illustrate the methodology employed in this study. The database is available as an electronic flatfile. Supporting information compiled in this study, such as electronic CPT data and detailed descriptions of the case histories, are also shared.*

KEYWORDS: case histories, CPT, free-field site, liquefaction, settlement.

SITE LOCATION: Geo-Database

INTRODUCTION

Free-field, level ground, liquefaction-induced settlement is a key mechanism of ground failure (e.g., Lee and Albaisa, 1974; Ishihara and Yoshimine, 1992; and Bray and Macedo, 2017). It can be treated as an index of ground damage due to liquefaction in the Pacific Earthquake Engineering Research (PEER) Center performance-based earthquake engineering framework (Deierlein et al., 2003). Liquefaction-induced ground settlement can damage infrastructure, such as buried utilities or lightweight structures with shallow foundations, as reported in the Marina District after the 1989 Loma Prieta earthquake (O'Rourke and Roth, 1990). The amount of ground settlement and the time it takes for the settlement to occur depend primarily on the subsurface soil conditions and the earthquake ground shaking.

The mechanisms of liquefaction-induced ground settlement are related to complex particle sedimentation and soil reconsolidation processes that occur during and after earthquake shaking. Sedimentation and reconsolidation occurring within a soil unit not easily captured by continuum-based numerical simulations. Hence, current engineering practice relies on semi-empirical models that are based on and validated against field case histories. Early models (e.g., Tokimatsu and Seed, 1987; Ishihara and Yoshimine, 1992) were developed considering a relatively small number of case histories, usually characterized with the standard penetration test (SPT). More recent models based on the cone penetration test (CPT) have been widely adopted because of the CPT's superior repeatability and nearly continuous profiling relative to the SPT. However, these methods (e.g., Zhang et al., 2002; Yoshimine et al., 2006; and Idriss and Boulanger, 2008) still suffer from being validated against a limited number of field case histories. Consequently, these procedures were developed deterministically with no quantification of the uncertainty of the liquefaction-induced ground settlement estimate.

Submitted: 24 September 2022; Published: 31 July 2023
Reference: Olaya, F. R., and Bray, J. D. (2023). Post-Liquefaction Free-Field Ground Settlement Case Histories. International Journal of Geoengineering Case Histories, Volume 7, Issue 3, pp. 18-33,
doi: 10.4417/IJGCH-07-03-02

Assessment of liquefaction-induced ground damage under performance-based frameworks provides valuable information for seismic design. In geotechnical engineering, robust probabilistic procedures for estimating post-liquefaction free-field settlements are required. The initial step in the development of these procedures is a comprehensive database of field case histories that represents sites of different formation processes, with uniform or interlayered stratigraphy, which were subjected to ground motions of different intensities and durations.

Obtaining field case histories with reliable pre- and post-earthquake ground elevation measurements is one of the primary limitations in the development of predictive models of liquefaction-induced settlement. CPT-based investigations and topographic surveys conducted by the United States Geological Survey (USGS) following the 1989 Loma Prieta earthquake produced some of the first CPT-based well-documented case histories of post-liquefaction settlement in the United States (U.S.). Additional case histories have gradually become available as records of land damage were made accessible after major earthquakes (e.g., 1999 Chi-Chi, Taiwan; and 2011 Tohoku, Japan). Reconnaissance efforts conducted in Christchurch, New Zealand (NZ), after the 2010-2011 Canterbury earthquake sequence have contributed much data related to ground motion recordings, patterns of seismic ground performance, and ground characterization, largely through CPTs, areal imagery, LiDAR measurements, and extensive subsurface characterization campaigns. The combination of this information provides a great opportunity to advance current empirical models. Research by the University of Canterbury, University of California - Berkeley, University of Texas at Austin, and Tonkin + Taylor produced an initial set of 55 well-documented sites with predominantly low levels of land damage (Russell and van Ballegoy, 2015; and Cubrinovski et al., 2019). Most of these sites correspond to locations where no-to-minor land damage was observed even though simplified liquefaction methods anticipated severe surface manifestations. An additional 34 sites were developed by Mijic et al. (2021) with the objective to include sites with and without liquefaction manifestations that show no major discrepancies between the estimates from simplified liquefaction methods and the actual field observations. Of these two sets of sites in Christchurch, those with free-field, level ground conditions were investigated further as part of this study. Field case histories in Wellington, NZ, from other recent earthquakes were also added.

The primary objective of this paper is to document field case histories of post-liquefaction free-field, level ground settlement. Because the CPT has become the preferred in-situ test in research and practice due to its higher reliability compared to the SPT (NRC, 2016), only case histories with CPT data available were collected. In addition to ground settlement data and soil profile information, CPT-derived parameters such as the soil behavior type index (I_c; Robertson, 2009a) are also documented. The characteristics of the ground motions associated with the case histories are documented through intensity measures (*IMs*) like the ground surface peak ground acceleration (*PGA*), 5%-damped spectral acceleration (S_a), cumulative absolute velocity (*CAV*), and Arias intensity (I_A). A *flatfile* containing the synthesis of parameters for each case history is provided as an electronic supplement in addition to the raw electronic CPT soundings (when publicly available) and appendices detailing each case history. These field case histories can be used subsequently in the development of new empirically-based probabilistic methods that account for the uncertainty in the settlement estimates to support performance-based earthquake engineering approaches.

PREVIOUS STUDIES

SPT-Based Case Histories

The landmark works of Tokimatsu and Seed (1987) and Ishihara and Yoshimine (1992) provided useful engineering procedures to estimate free-field post-liquefaction ground settlement based on SPT data. Their procedures are rooted in laboratory-based relationships between the relative density (D_r), the factor of safety against liquefaction triggering (FS_L), and reconsolidation volumetric strains (ε_v). Ishihara and Yoshimine (1992) used 6 SPT case histories from the 1964 Niigata, Japan, moment magnitude (M_w) 7.5 earthquake to evaluate the reliability of their procedure. The Niigata sites are predominantly sand deposits with a few localized thin silt lenses. A *PGA* of 0.16 *g* recorded at a nearby strong motion station was assumed to be representative of the seismic demand at the sites (Ishihara and Yoshimine, 1992).

Wu and Seed (2004) developed a ground settlement procedure based on cyclic tests performed on Monterey 0/30 sand. In contrast to Ishihara and Yoshimine (1992), their model uses a $M_w = 7.5$ cyclic stress ratio ($CSR_{7.5}$) as a demand term and the overburden-corrected, energy-corrected, clean sand equivalent blow count, $(N_1)_{60,cs}$, as the resistance term. A total of 14 SPT case histories from 7 earthquakes were collected to validate their model. However, in their database they included the Moss Landing site that experienced lateral spreading in the 1989 Loma Prieta earthquake (Kayen and Mitchell, 1997). Thus, this case history was affected by lateral deformation in addition to free-field reconsolidation settlement.

Cetin et al. (2009) expanded the Wu and Seed (2004) laboratory clean sand data to develop a probabilistic post-liquefaction ground settlement model. In this model, the demand term is defined as CSR_{field} which is the CSR corrected for magnitude, unidirectionality of shaking, and atmospheric pressure, while $(N_1)_{60,cs}$ is kept as the resistance term. For model validation and additional regression analyses, 49 well-documented SPT case histories were collected. They also used these case histories to quantify the variability in the settlement estimate. Some of the case histories in Cetin et al. (2009) are reported to have been also affected by lateral displacements in the range of 200 mm to 600 mm.

Recently, Mesri et al. (2018) developed a predictive model that depends on the coefficient of vertical compression (m_{vs}) and the excess pore-water pressure generated by the earthquake (u_g). These parameters are formulated as a function of the energy-corrected SPT blow count N_{60} and FS_L. For validation, they used ground settlement observations from 78 case histories from earthquakes with M_w between 7.1 and 8.0, and PGA ranging from 0.16 g to 0.35 g.

The number of SPT case histories of post-liquefaction free-field ground settlement have grown from less than 10 to almost 80 over the last three decades as a result of different research efforts following important earthquake events. Despite these advancements, borehole logs with well-documented, reliable SPT data are not readily available and differences between the interpretation of the case histories among the different studies exist. Also, the SPT case histories discussed previously are largely influenced by data from the 1989 Loma Prieta and 1995 Hyogoken Nambu earthquakes. These two events contribute with 80% and 70% of the total number of case histories in the Cetin et al. (2009) and Mesri et al. (2018) databases, respectively.

CPT-Based Case Histories

Zhang et al. (2002) adapted the Ishihara and Yoshimine (1992) relationship between the factor of safety against liquefaction and reconsolidation volumetric strains to develop a widely used CPT method for estimating liquefaction-induced ground settlement. As part of the study, they developed case histories in the Marina District and Treasure Island after the M_w 6.9 1989 Loma Prieta earthquake to validate their method. A total of 11 sites were documented and interpreted. These sites generally consist of hydraulic sandy fill on top of natural sand deposits that overly clay deposits and experienced $PGAs$ between 0.12 g to 0.24 g.

Juang et al. (2013) expanded the work of Zhang et al. (2002) by including the probability of liquefaction into the model formulation and by extending the number of free-field settlement case histories to 32. Many sites investigated following the 1999 Chi-Chi earthquake were added to the cases previously reported by Zhang et al. (2002). The Chi-Chi case histories supplies data with recorded $PGAs$ up to 0.79 g, which adds valuable information to the range of $PGAs$ covered by previous case histories. Juang et al. (2013) also reported 32 additional "building case histories" (i.e., cases where the settlement is influenced by building movement).

Sadeghi et al. (2021) performed a series of numerical analyses assuming different soil conditions and ground motion parameters to develop a synthetic dataset of post-shaking settlement. This synthetic dataset was then used as the basis for a functional predictive model. Their model was subsequently compared with 32 free-field ground settlement case histories. Similar to the SPT case histories discussed previously, the CPT case histories presented by Sadeghi et al. (2021) show an important overlap with previous studies (e.g., Juang et al., 2013) with the main addition by Sadeghi et al. (2021) being the inclusion of 6 case histories from the 2010-2011 Canterbury earthquake sequence in Christchurch.

Figure 1 shows the growth of the number of SPT and CPT case histories over the last three decades (including the number of case histories added in this study). Before this study, the number of CPT case histories of post-liquefaction free-field ground settlement was less than half of the number of the SPT cases, despite the superiority of the CPT in characterizing the ground relative to the SPT. Additionally, previous liquefaction-induced ground settlement databases do not provide a clear definition of what constitutes a field case history. From the cases discussed previously, it appears that many of the case histories have been defined using a single CPT. This is potentially problematic because closely spaced CPTs are correlated and should not be treated as independent case histories. Moreover, the spatial variability of a site cannot be evaluated if there is only one CPT defining the ground conditions at a site.

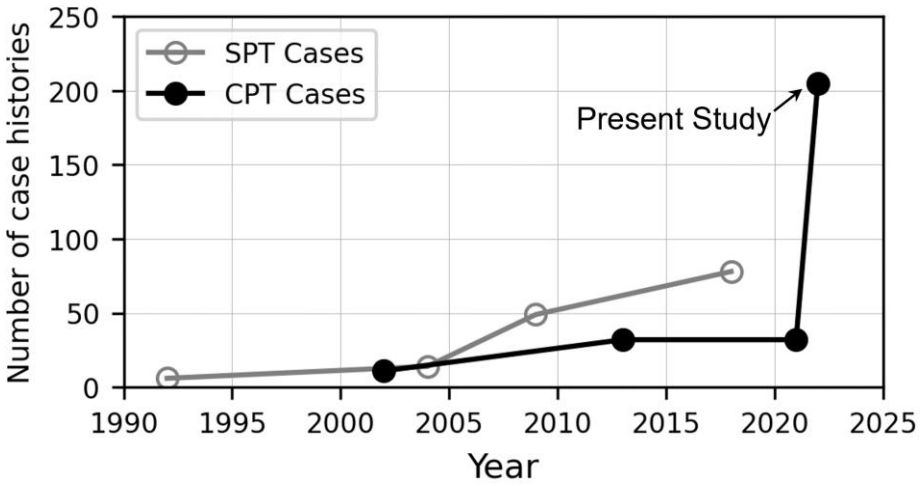

Figure 1. Increase of liquefaction-induced ground settlement field case histories.

CASE HISTORIES AND DATA DOCUMENTATION

Post-Liquefaction Ground Settlement Case History Definition

The field case histories developed for this study are a collection of subsurface geotechnical data derived mainly from surficial geological information and CPT penetration data; groundwater depth; observations of field performance in the form of pre- and post-event topographic surveys, LiDAR data, or satellite imagery; and characterization of the ground motion associated to the occurrence of liquefaction at the site. In addition to M_w, earthquake ground shaking in liquefaction evaluations is commonly represented by intensity measures (*IMs*) such as *PGA*, S_a, *CAV*, or I_A. Obtaining field case histories with reliable pre- and post-earthquake ground surface elevation measurements is the primary limitation in the development of post-liquefaction ground settlement case histories.

In this study, a case history is defined as the combination of: (1) a site with laterally consistent soil stratigraphy with at least one CPT, (2) an earthquake event represented by its M_w, ground surface *PGA,* or other intensity measures, and (3) consistent post-liquefaction volumetric-induced free-field, level ground settlement measurements. A site is not defined by a CPT. Instead, a site is defined by its consistent geology and seismic performance. Thus, each case history is a site characterized by a geometric mean set of CPT-derived parameters, which undergoes an estimated level of earthquake shaking, wherein the liquefaction-induced ground settlement was measured. Sites characterized by several CPTs are valuable as they capture the average subsurface conditions and the variability of the CPT parameters across a site. For sites with multiple CPT soundings or multiple point settlement measurements, geometric means of these values are used to represent central values in the case history.

Case History Descriptions

Well-documented field case histories provide valuable information about the interaction effects of variable soil properties, stratigraphy, and multi-directional shaking. This information is key for developing robust empirical models (e.g., Bray et al., 2017). In the context of developing an empirical model, ground motion *IMs* have been used successfully (e.g., Bray and Macedo, 2017; Bullock et al.´, 2019) with representative soil parameters and site conditions presented in the form of soil types captured by indices such as the soil behavior type index (I_c, Robertson, 2009a), relative density (D_r), or the state parameter (ψ_o, Been and Jefferies 1985). Before presenting the methodology used to generate the selected *IMs* and soil parameters, a brief description of the site characteristics of the case histories is presented as it provides the necessary background for interpretation of these case histories. In addition, sources of CPT and other field data are given.

Post-earthquake reconnaissance efforts by Bennett (1990), Power et al. (1998), and Hryciw (1991) are the source of the subsurface geotechnical characteristics and post-liquefaction settlement data for the Marina District and Treasure Island sites following the 1989 Loma Prieta earthquake. The Marina District is an 8 m to 10 m thick hydraulic fill site composed of clean to silty sands (SP, SP-SM) with fines content (*FC*) up to 21%. Underlaying the sandy fill is the San Francisco Young Bay

Mud clay deposit. Treasure Island is a hydraulic fill located 6.5 km from Marina District. It consists of an 8 m thick, clean to silty sand fill followed by a shoal sand unit of similar thickness overlying the San Francisco Young Bay Mud deposit. The fill and shoal are of similar gradation (*FC* up to 40%) but the shoal deposit shows some clay bridging of particles, particle interlocking, and other fabric effects.

CPT raw data were obtained from the USGS (2021a)/Holzer et al. (2010), the Next Generation Liquefaction Project (NGL, Zimmaro et al., 2019, accessed 2021), and from ENGEO (2015, 2019a, 2019b, and 2019c). With the geotechnical and topographic data and the available CPTs, 4 and 5 case histories were defined in the Marina District and Treasure Island, respectively, for the 1989 Loma Prieta earthquake.

Juang et al. (2002) summarized findings from the reconnaissance mission of the Taiwanese National Center for Research in Earthquake Engineering (NCREE) in the cities of Yuanlin and Wufeng. Lee et al. (2011) and Chu et al. (2003) performed additional ground investigations and topographic surveys. Their results provide information about the geotechnical characteristics and post-liquefaction settlement for the Yuanlin and Wufeng sites after the 1999 Chi-Chi, Taiwan, earthquake. The Yuanlin site is composed of a series of fine silty sand layers of variable *FC* and silt layers with occasional clay lenses. The soil in Wufeng is composed of layers of silty sand, sandy silt, and silty clay up to a depth of about 20 m. The fine fraction of the soils at the Wufeng sites have a plasticity index (*PI*) typically less than 7 (Lee et al., 2011). CPT data were obtained from the investigation campaigns documented by Chu et al. (2004) and Juang (2002). Based on this information, 3 case histories were defined in Yuanlin and 3 other cases in Wufeng for the 1999 Chi-Chi earthquake.

The stratigraphy, soil types, and the effects of liquefaction experienced at CentrePort in Wellington after the 2013 Cook Strait, 2013 Lake Grassmere, and 2016 Kaikoura earthquakes have been documented extensively in the studies by Cubrinovski et al. (2018), Bray et al. (2019), Dhakal et al. (2020), and Dhakal et al. (2022). CentrePort is a 10 m to 20 m thick hydraulic fill where the first 2 m to 3 m correspond to a compacted layer (crust) generally above the groundwater level. An older reclamation constructed in 1910s was constructed by placing a 1 m to 7 m thick layer of a gravel-sand-silt mixture which overlies 1 m to 6 m of gravelly sand. The most recent reclamation (i.e., the Thorndon reclamation) consists of 10 m of sandy gravel fill below the crust. For both types of fills, the sandy gravel and gravel-sand-silt mixtures, the sand and silt fractions make up between 20% and 50% of the fill. Following the fill materials, uncompacted marine sediments of 1 m to 4 m of thickness and composed of clays, silty clays, and sands are found. CPT data have been shared through a research effort led by the Univ. of Canterbury in collaboration with the Univ. of California – Berkeley, Tonkin + Taylor, Ltd., and CentrePort. At the time of this paper's authoring, the electronic data, which was available for this study, have not been not approved by CentrePort to be released publicly. However, much of the information is available to the public through the publications mentioned previously. A total of 27 case histories have been developed for CentrePort for primarily the 2016 Kaikoura and 2013 Lake Grassmere earthquakes, with one case for the 2013 Cook Strait earthquake.

The Christchurch liquefaction vulnerability study by Tonkin + Taylor (Russell and van Ballegoy, 2015) documented and investigated land damage throughout Christchurch after the 2010-2011 Canterbury earthquake sequence. As a result, a set of well-documented 55 sites with varying levels of ground damage was defined and used to study liquefaction triggering and its effects (Cubrinovski et al., 2019). Mijic et al. (2021) complemented the existing 55 sites with 34 additional sites to arrive at an unbiased set of sites with levels of liquefaction manifestations from none-to-severe. The set of 89 sites in Christchurch can be broadly classified into sites of relatively continuous (thick) sandy materials and sites with different degrees of stratification with presence of interbedded sandy, silty, and clayey materials (Beyzaei et al., 2018). These surficial sand, silt, and gravel deposits vary in thickness from less than 10 m to over 40 m in the northern and eastern part of Christchurch, whereas swamp deposits of the same thickness and composed of sand, silt, clay, and peat are in the southwestern part of the city. Underlying these soils, a sequence of thick layers of gravels and sands with silts are found (Markham et al., 2016). High-quality pre- and post-earthquake LiDAR surveys data, CPT recordings, and soil boring logs were obtained from the New Zealand Geotechnical Database (2021). Information for the 2010 Darfield, 2011 Christchurch, and June 2011 earthquakes were processed to develop a total of 157 case histories in Christchurch.

Tokimatsu et al. (2012) and Kokusho et al. (2014) document field data of the hydraulic fills in Urayasu, Japan. The reclaimed land of Urayasu is an 8 m thick hydraulic fill composed of loose silty sands and sandy silts that sit atop a soft to firm clay stratum about 10 to 40 m thick. Information regarding the overall seismic performance and the range of observed settlements in Urayasu are provided in Katsumata and Tokimatsu (2012) and Cox et al. (2013). In addition to providing ranges of free-field ground settlement, Cox et al. (2013) shows CPT data at 6 different locations in Urayasu. With this information, 6 case histories are developed for the Urayasu sites shaken by the 2011 Tohoko earthquake.

Initially 213 case histories were collected, processed, and examined. Through closer examination, 6 cases were removed from the database because they were potentially affected by liquefaction-induced lateral ground movements due to buried stream channels or buried structures such as pools. Preliminary regression analysis of the settlement data of the remaining cases identified 2 outliers that were more than 3 standard deviations from the median of the regression of the data. Simplified liquefaction triggering procedures indicated these 2 cases were marginal liquefaction cases, so they were removed.

The final database contains 205 case histories with 967 CPTs. Table 1 summarizes the characteristics of the assembled 205 CPT case histories of post-liquefaction free-field, level ground settlement. Each case history is described in detail in a *flatfile* shared as an electronic supplemental document, which includes the latitude and longitude of each site. The publicly available electronic CPT data and the details of each field case history are also available as electronic supplements.

Reclaimed land is typically the product of sequential hydraulic filling of borrowed granular material. This construction method results in relatively uniform and loose fills typically overlying marine sediments. The hydraulic fills in the database are usually less than 10 m thick and are typically comprised of silty sands to sandy silts (with exception of CentrePort, which has a significant fraction of gravel). Case histories of the performance of hydraulic fills, such as those during the 1995 Kobe earthquake (e.g., Yasuda et al., 1996), indicate that uniformly constructed hydraulic fills tend to exhibit relatively uniform settlement. Conversely, natural soil deposits are inherently heterogenous as a consequence of complex depositional processes that can show significant spatial variability in addition to other age-related effects. The assessment of liquefaction performance in the Christchurch (Beyzaei et al., 2018) illustrates the effects of depositional processes on ground performance. Due to the differing formation processes and their seismic response, the case histories are classified into the two primary categories of natural soil deposits and hydraulic fills. Of the 205 case histories, 163 cases are classified as natural soil deposits and 42 cases are classified as hydraulic fills.

Table 1. Summary of Free-Field Settlement Case Histories (See supplemental flatfile for additional information.)

Location	Earthquake	Case histories	CPTs	Type of deposit
Marina District, California	1989 Loma Prieta	4	8	Hydraulic fill
Treasure Island, California		5	84	
Wufeng, Taiwan	1999 Chi-Chi	3	3	Natural soil
Yuanlin, Taiwan		3	4	
CentrePort, Wellington	2013 Cook Strait	1	8	Hydraulic fill
	2013 Lake Grassmere	13	69	
	2016 Kaikoura	13	69	
Christchurch, New Zealand	2010 Darfield	45	210	Natural soil
	2011 Christchurch	47	220	
	2011 June	65	285	
Urayasu, Japan	2011 Tohoku	6	6	Hydraulic fill

CPT Data

The raw electronic CPT profiles were evaluated before being processed. CPTs with the following characteristics were not used in this study:

a) CPTs with incomplete data (e.g., missing data in the upper 10 m of the profile below the groundwater level),

b) Very short CPT profiles (i.e., ≤ 5 m depth of penetration), and

c) Trace of a CPT differed markedly from the traces of the other CPTs at the site.

Figure 2 shows an example of an excluded CPT (i.e., CPT 56472 shown in red) with normalized tip resistance (q_{c1N}) and I_c profiles markedly different from the q_{c1N} and I_c profiles of the other CPTs defining the Shirley Intermediate School site. CPT 56472 defines the northern edge of the Shirley Intermediate School site, as it contains noticeably more gravel and is significantly denser than the soil profiles described by the other CPTs located closer to the center of the site.

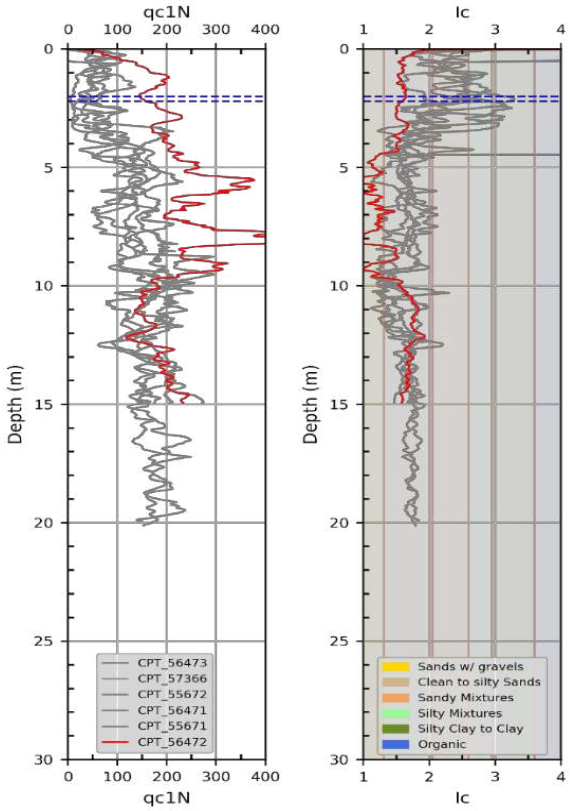

Figure 2. Example of an excluded CPT at a site (CPT 56472 in red at the Shirley Intermediate School site).

Groundwater Depth

Groundwater table (GWT) depths at CPT locations in the Marina District were estimated by Bennett (1990) from boring logs. A mean GWT depth of 2.90 m is representative of the site with exception of the southeast area, where a GWT depth of 5.40 m is more representative. The GWT in Treasure Island is related to the sea mean lower low water (MLLW). At the time of the 1989 Loma Prieta earthquake, the GWT depth was estimated between 0.90 m and 2.0 m. Juang et al. (2002) reports GWT depth estimated by the NCREE reconnaissance effort. Depths of 0.5 m to 4.0 m and 0.5 m to 5.0 m are estimated in Yuanlin and Wufeng, respectively, at the time of the 1999 Chi-Chi earthquake. An analysis of piezometer data in CentrePort by Dhakal et al. (2020) indicates that the GWT depth varied between 2.0 m and 4.0 m during the 2013-2016 earthquake sequence. In Christchurch, event-specific GWT depths have been obtained from wells installed prior to and after the Darfield 2010 earthquake combined with LiDAR data. The GWT levels in the wells measured prior to the Christchurch 2011 and June 2011 events were used to generate surfaces of GWT depth for these earthquakes. Lastly, similar to other hydraulic fills, the GWT depth in the Urayasu site is relatively uniform and varies within 0.5 m to 3.0 m (Tokimatsu et al., 2012)

Derivation of CPT-Based Parameters

Each CPT sounding provides corrected cone resistance (q_t often also referred to as q_c in the literature), sleeve friction (f_s), and dynamic pore pressure (u_2) measurements. The combination of these measurements permits the interpretation of the stratigraphy and characterization of soil behavior type index with depth. In addition, there exist several mechanistically based correlations that relate cone measurements to different soil properties and parameters (e.g., relative density and peak effective friction angle). The ability to obtain reliable estimates of engineering soil properties is one of the major advantages of the CPT in engineering practice.

The soil behavior type index is a useful CPT-derived parameter. It classifies the soil based on the in-situ type of response during shearing (e.g., sand-like or clay-like, and loose or dense). In addition, an $I_c = 2.6$ threshold is typically adopted in simplified liquefaction triggering methods to identify soils with $I_c \geq 2.6$ as non-liquefiable. The I_c relationship proposed by Robertson (2009a) as shown in Eq. 1 is used in this study.

$$I_c = [(3.47 - \log Q_t)^2 + (\log F_r + 1.22)^2]^{0.5} \quad (1)$$

where the normalized tip resistance, $Q_t = (q_t - \sigma_v) / \sigma'_v$; the normalize friction ration, $F_r = f_s/(q_t - \sigma_v)$; and σ_v and σ'_v are the total and effective vertical stresses, respectively.

An estimate of *FC* is also required in routine triggering methods as well as in other informative correlations. Idriss and Boulanger (2008) recommend measuring the *FC* directly from representative samples; however, this may not be practical in many engineering applications. Even though discrepancies between I_c and *FC* classifications are expected (e.g., Robertson, 2009a; and Beyzaei et al., 2018b), correlations between I_c and *FC* have been proposed and implemented in practice and research. The *FC* (in %) relationship of Boulanger and Idriss (2014) as shown in Eq. 2 is used in this study.

$$FC = 80(I_c + C_{FC}) - 137 \quad (2)$$

where C_{FC} is a calibration parameter that is set to zero to obtain a global average relationship. If site-specific data are available, a material-specific calibrated C_{FC} can be used. For example, Maurer et al. (2019a) evaluated many field samples and CPT data and suggested using $C_{FC} = 0.13$ for the soil deposits in Christchurch.

The CPT data can also be used to obtain estimates of soil state. Relative density (D_r) and the state parameter (ψ_o) are used in this study. D_r (in %) is estimated using the correlation developed by Bray and Olaya (2023) defined in Eq. 3, which is based on data at natural silty sand deposits in Christchurch in which high-quality samples were retrieved only 1 to 2 m from a CPT that defined the normalized cone resistance (q_{c1n} as defined by Boulanger and Idriss, 2014) and I_c over well-defined soil layers. As an alternative to this new correlation, the Robertson and Cabal (2015) CPT-based D_r (in %) correlation for clean sand defined in Eq. 4 is used by extending it to capture silty soil with $I_c > 1.64$ through application of the clean sand correction factor (K_c) of Robertson and Wride (1998).

$$D_r = \begin{cases} \sqrt{\frac{q_{c1n}}{290}} \cdot 100 & \text{for } I_c < 1.6 \\ \sqrt{\frac{q_{c1n} \cdot I_c^{3.5}}{1500}} \cdot 100 & \text{for } 1.6 \leq I_c \leq 2.6 \end{cases} \quad (3)$$

$$D_r = \sqrt{\frac{Q_{tn,cs}}{350}} \cdot 100 \quad (4)$$

where the normalized clean-sand-equivalent cone resistance, $Q_{tn,cs} = K_c \cdot Q_{tn}$, $K_c = 5.581 I_c^3 - 0.403 I_c^4 - 21.63 I_c^2 + 33.75 I_c - 17.88$ if $I_c > 1.64$, and Q_{tn} is the normalized CPT penetration resistance as defined by Robertson and Cabal (2015).

The Robertson and Cabal (2015) correlation was developed based on clean sand data from calibration chamber tests. The $Q_{tn,cs}$ term permits extending the application of the correlation to silty sands by means of the clean-sand-equivalent resistance correction. In contrast, the Bray and Olaya (2023) correlation was developed directly using closely spaced high-quality CPT and laboratory test data on clean and silty sands in Christchurch (i.e., Markham, 2015; and Beyzaei, 2017); hence, a clean-sand-equivalent correction is not needed. However, both correlations use normalized cone resistance and soil behavior type index values to estimate relative density. The average of both relationships is used in this study to use an unbiased mean-centered estimation of D_r. Figure 3 shows the *FC* and D_r correlations employed in this study.

The state parameter (ψ_o in decimal) is estimated using the correlations of Robertson (2010), which is provided in Eq. 5, and of Olaya and Bray (2022), which is provided in Eqs. 6 and 7.

$$\psi_o = 0.485 - 0.314 \cdot \log Q_{tn,cs} \quad (5)$$

$$\psi_o = \xi \cdot (e_{max} - e_{min}) \left[1/\mathrm{Ln}\left(\sigma'_{cr}/\sigma'_v\right) - D_{r_o}\right] \quad (6)$$

$$\xi = 0.724 \cdot \exp(-0.031 \cdot FC) \quad (7)$$

where ξ is a calibration parameter, (e_{max} - e_{min}) is the void ratio range of the soil, σ'_{cr} is the crushing pressure, σ'_v is the vertical effective stress, and D_{r_o} is an estimate of the initial D_r expressed in decimal. Examination of Eq. 6 showed the estimate of ψ_o is not too sensitive to σ'_{cr}, so typical values provided by Mitchell and Soga (2005) may be used (i.e., 8000 kPa for silt; 10000 kPa for silty sand; and 20000 kPa for clean sand). The average of the soil-dependent correlation of Cubrinovski and Ishihara (2002) is used to estimate $e_{max} - e_{min}$ as

$$e_{\max} - e_{\min} = \begin{cases} 0.43 + 0.00867 \cdot FC, & FC < 30 \\ 0.57 + 0.004 \cdot FC, & FC \geq 30 \end{cases} \quad (8)$$

where FC is expressed in percent as an integer. Typical values of $e_{max} - e_{min}$ are 0.45 for clean sand, 0.65 for silty sand, and 0.80 for silt.

The Robertson (2010) correlation for ψ_o has been derived based on clean sand data and it is extended to silty sands through the use of $Q_{tn,cs}$. The Olaya and Bray (2022) relationship is based on critical state theory concepts and was calibrated using laboratory test data on clean and silty sands. The average of both correlations is used as a representative mean estimate in this study.

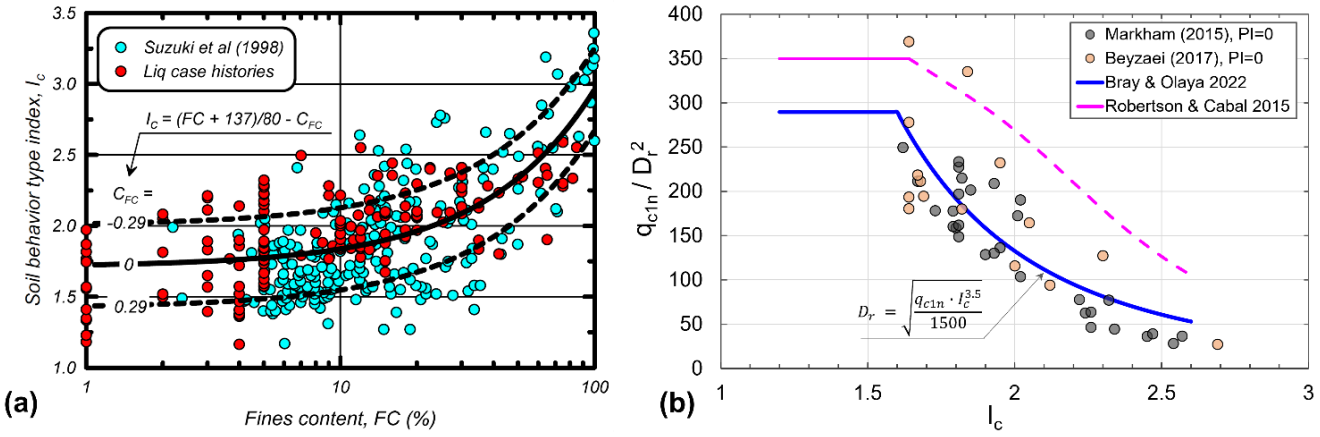

Figure 3. CPT-based (a) fines content correlation of Boulanger and Idriss (2014), and (b) relative density correlations of Bray and Olaya (2023) for natural soil deposits and inferred from Robertson and Cabal (2015).

Liquefaction Triggering Evaluation

Two simplified liquefaction triggering methods were used to compute the factor of safety against liquefaction (FS_L). Within each triggering method, a probability of liquefaction, P_L = 50% was used so that median estimates of FS_L are obtained. The methods of Boulanger and Idriss (2014) and Robertson and Wride (1998) with the modifications in Robertson (2009b) were used. While the Boulanger and Idriss (2014) method is also provided in a probabilistic framework, the Robertson and Wride (1998) is not. The work of Ku et al. (2012) was used to adjust the Robertson and Wride (1998) method to achieve P_L = 50%. The average of the median (P_L = 50%) FS_L estimates of Boulanger and Idriss (2014) and of Robertson and Wride (1998)/Robertson (2009b)/Ku et al. (2012) is used in the database.

Ground Motion Intensity Measures and Liquefaction Severity Indexes

The seismic demand at case histories sites is represented with surface ground motion intensity measures (e.g., *PGA*, and S_{a1} = S_a at a period of T = 1 s). At sites with ground motion recordings available from nearby stations (e.g., CentrePort), *IMs* derived from the recordings are used. When no ground motion recordings were available in the vicinity of the site, average median estimates obtained from ground motion models (GMMs) for S_a are used. For the Christchurch sites, the Bradley (2014) procedure was used to estimate values of *PGA* and S_{a1} conditioned on observed spectral accelerations at strong motion

stations throughout Christchurch. For sites without an event-specific GMM, the NGA-West2 set of models (Gregor et al., 2014) were used.

The time-averaged 30 m soil shear wave velocity (V_{S30}) is commonly used as a site parameter describing the near-surface soil conditions in GMMs, so V_{s30} values are provided for all case histories. Direct measurements of V_s at the sites are limited. McGann et al. (2017) used V_s and CPT measurements throughout Christchurch to develop a Christchurch-specific empirical model for V_{s30}. Vantassel et al. (2018) used the multichannel analysis of surface wave (MASW) and microtremor array measurements (MAM) to develop V_s profiles in CentrePort. Cox et al. (2013) provide V_s measurements at the 6 different locations where they advanced the CPTs in Urayasu. Liu et al. (2015) used the measured V_{s30} from the dense Taiwanese strong motion station array to estimate V_{s30} at locations in Taiwan. Similarly, USGS (2021b), and the California Department of Conservation (2021) developed estimates of V_{s30} using V_s measurements for the Marina District and Treasure Island sites. Site-specific V_s and V_{s30} data were used when available instead of generic CPT correlations for V_s.

In simplified liquefaction triggering assessments, M_w is used as a proxy for shaking duration effects while horizontal ground surface *PGA* defines the ground motion intensity at the site. Research on the effects of liquefaction (e.g., Bray and Macedo, 2017; and Bullock et al., 2019) have shown that the spectral acceleration at a degraded period of the site, T' ($S_{aT'}$), *CAV*, and I_A have good potential as ground displacement predictor variables, hence they are also included. To estimate *CAV* and I_A, this study employs the GMMs of Campbell and Bozorgnia (2012), Abrahamson et al. (2016), and Macedo et al. (2021) for shallow crustal regions and the GMMs of Foulser-Piggott and Goda (2015) and Macedo et al. (2019) for subduction zone earthquakes. Figure 4 presents the distribution of V_{s30} and the ground motion *IMs* developed for the database of this study.

Liquefaction-induced ground damage severity indexes have been developed to relate the FS_L to the degree of observed ground damage. Previous research (e.g., Maurer et al., 2014; and Hutabarat and Bray, 2021) have shown that the accuracy of different liquefaction indices depends greatly on the site's stratigraphy and the site's system response to earthquake shaking. Therefore, it is informative to include relevant liquefaction indices as part of the case histories development so that the correspondence between liquefaction-induced ground settlement and different liquefaction indices can be explored. The Liquefaction Index Potential (*LPI*), the Ishihara-inspired LPI (LPI_{ish}), and the Liquefaction Severity Number (*LSN*) were computed in this study (each index is defined in Maurer et al., 2019b). In addition, the Liquefaction Demand parameter (L_D) and the Crust Resistance parameter (C_R) as defined by Hutabarat and Bray (2022) are also provided for each site.

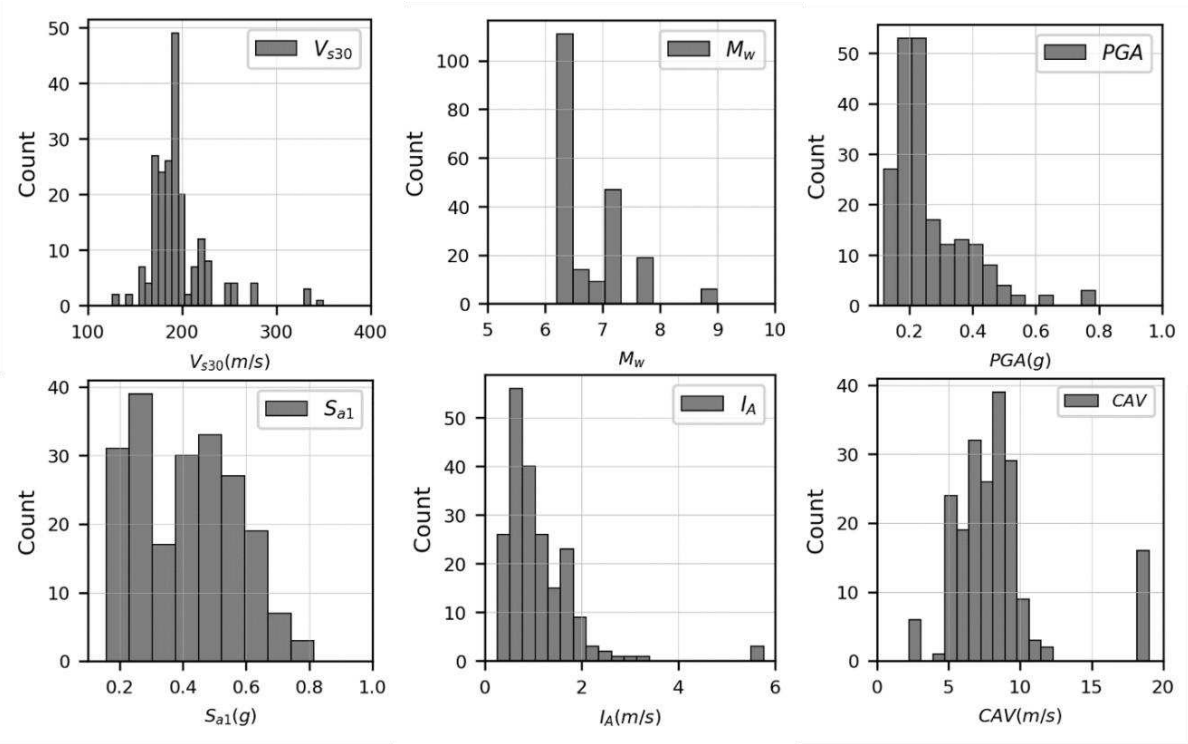

Figure 4. Distribution of V_{s30} and key Intensity Measures in the database.

Free-Field Ground Settlement Measurement

Vertical ground settlement in the Marina District after the 1989 Loma Prieta earthquake was estimated by Bennett (1990) as the difference in elevation from surveys conducted in 1961, 1974, and 1989 (post-earthquake). The settlement component due to compression of the bay mud and consolidation of the fill was assessed using the difference between the 1961 and 1974 surveys. At first, the 1974 – 1961 settlement was planned to be subtracted from the 1974 – 1989 settlement to isolate the earthquake induced settlement. However, Bennett (1990) pointed out that many uncertainties were not captured by the topographic surveys; hence, it was recommended to use the settlement between 1974 and 1989 as the post-earthquake settlement because it could provide an estimate that accounts for these uncertainties. For Treasure Island, the settlement after the 1989 Loma Prieta earthquake was estimated by Bennett (1998) using topographic survey data at a few free-field locations that were next to pile supported buildings assumed not to have settled due to the earthquake.

For the Yuanlin and Wufeng sites, land subsidence measurements after the 1999 Chi-Chi earthquake were conducted by the Taiwanese National Center for Research in Earthquake Engineering (NCREE), and are documented in Juang (2002) and Juang et al. (2013). Lee et al. (2011) discusses additional ground settlement measurements that were carried out in 2005 employing GPS surveys, reconnaissance reports, and site photographs for the Wufeng area. These two survey campaigns were used to estimate the post-liquefaction ground settlement at sites in Yuanlin and Wufeng.

Ground settlement at CentrePort following the 2013 Cook Strait and 2013 Lake Grassmere earthquakes was estimated primarily by manual field surveys as part of damage inspection campaigns. Settlement measurements are limited for the 2013 Cook Strait event, while for the 2013 Lake Grassmere settlement estimates are available for several locations. Shortly after the 2016 Kaikoura earthquake, ground settlements were documented from manual surveys. Later, terrestrial and areal LiDAR surveys were conducted in CentrePort and subsequent point estimates of settlement were calculated (Cubrinovski et al., 2018). Using these point measurements, settlement contours covering the CentrePort area were developed and shared in Dhakal et al. (2022). The latter, more precise settlement data were used in this study.

In Christchurch, LiDAR point cloud data were processed with Global Mapper to generate elevation models for total settlement, tectonic movement, and net ground subsidence (Mijic et al., 2021). These elevation models were further complemented with flight error estimates and localized ejecta-induced settlements. These LiDAR-based elevation models form the basis of the post-liquefaction ground settlement estimates after the 2010 Darfield, 2011 Christchurch, and June 2011 earthquakes.

Katsumata and Tokimatsu (2012) report the amount of ground settlement following the 2011 Tohoku earthquake. For these case histories, ground settlement was carefully measured at multiple locations using pile-supported structures that showed no evidence of displacement as a reference. These point-based measurements were later used to develop a map of post-liquefaction ground settlement.

The more densely surveyed areas, such as Marina District and Christchurch, provide insights into the range in which the ground settlement varies. Accordingly, a mean value and range of settlement were estimated based on field measurements, soil characteristics, and the degree of liquefaction observed at the site.

EXAMPLE OF THE DEFINITION OF A CASE HISTORY

Figure 5 illustrates the definition of a case history in CentrePort, Wellington. This case history corresponds to the performance at Site 4 after the 2016 Kaikoura M_w 7.8 earthquake. Site 4 is within a part of CentrePort built with dumped sandy gravel fill of thickness from 10 m to 15 m which overlies marine sediments and the Wellington alluvium. The sand-silt fractions of the gravelly fill range between 30% and 70%. Additional information on the stratigraphy, soil types, and the effects of liquefaction after the 2016 Kaikoura earthquake are available in Cubrinovski et al. (2018), Dhakal et al. (2020), and Dhakal et al. (2022). Site 4 is characterized by the 6 CPTs shown in Figure 5, with the groundwater table located between 3.0 m to 3.5 m below the ground surface. The CPT data (e.g., q_{c1n} and I_c) and liquefaction parameters (e.g., FS_L and LSN) were used to define the extent of a site. They are relatively consistent for the 6 CPTs advanced at Site 4. The average of the D_r estimated using Eq. 3 and Eq. 4 varies between 30% and 95% for this site, and the average of the P_L = 50% FS_L estimated using the Boulanger and Idriss (2016) and Robertson and Wride (1998)/Robertson (2009)/Ku et al. (2012) procedures vary between 0.30 and 2.0. The surveyed mean ground settlement varies within the range of 200 mm to 350 mm across most of the site. Lastly, the *PGA* at nonliquefied ground surface conditions was estimated to be 0.25 *g* with nearby strong motion stations that are not affected by liquefaction.

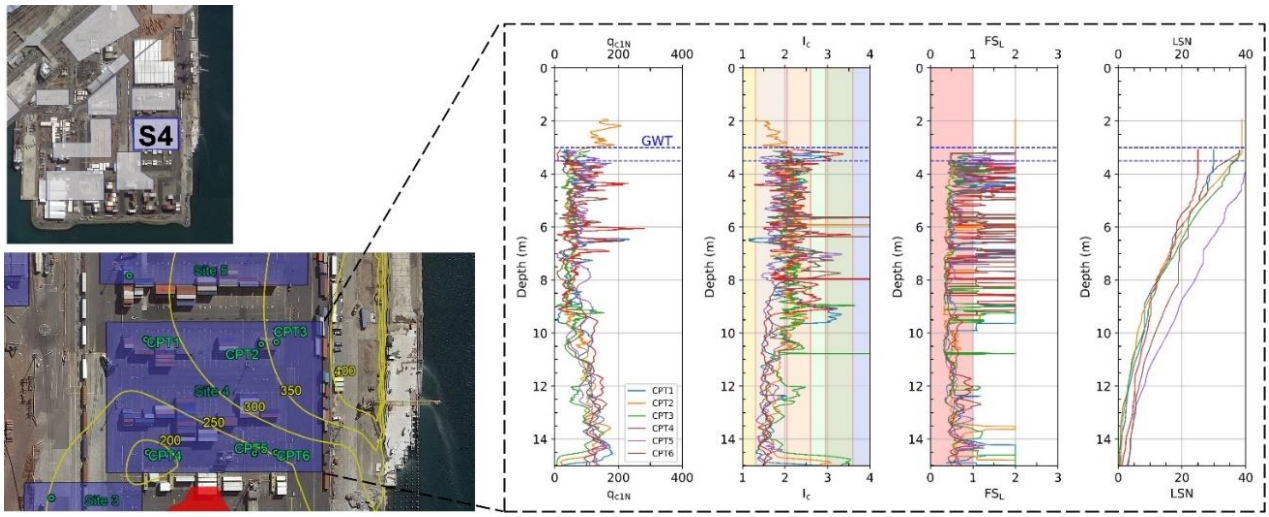

Figure 5. CentrePort with enlarged image of Site 4 showing CPT locations and mean ground settlement (mm) contours with q_{c1n}, I_c, FS_L, and LSN profiles. Images from Google Earth®.

CONCLUSION

A comprehensive database of 205 CPT field case histories of post-liquefaction free-field ground settlement has been developed. The case histories are classified into 163 natural soil deposit sites and 42 hydraulic fill sites, because these sites differ in their formation processes and spatial variability.

As part of the case histories characterization, a total of 966 CPTs were processed using several state-of-the-practice correlations and liquefaction triggering procedures. The in-situ state of the soil was characterized using the correlations of Robertson and Cabal (2015) and Bray and Olaya (2023) for the relative density, and Robertson (2010) and Olaya and Bray (2022) for the state parameter. The simplified liquefaction triggering methods of Boulanger and Idriss (2014) and Robertson and Wride (1998)/Robertson (2009b)/Ku et al. (2012) were employed. The use of at least two relationships for these key parameters provides mean-centered estimates of soil properties and liquefaction triggering.

The seismic demand associated with each case history is reported by means of the earthquake moment magnitude and a series of intensity measures that have been shown to correlate well with earthquake-induced ground and building displacements. Ground motion recordings were used directly to derive intensity measures at sites with nearby recordings available whereas for sites with no ground motion recordings, mean estimates from ground motion models were used. V_{s30} values are also provided for each case history because to provide an index for site response amplification, as typically used in modern ground motion models.

Best estimates of liquefaction-induced free-field settlement measurements are provided for each case history. The estimation of post-liquefaction settlement is difficult because in addition to the site's intrinsic spatial variability, there always exists uncertainty in the pre- and post-earthquake ground elevation surveys. Hence, for each site, a mean of settlement was estimated based on the topographic measurements, soil characteristics, and the degree of liquefaction observed at the site. To complement the mean settlement estimate, a range of the ground settlement is also provided.

ACKNOWLEDGMENTS

This research was supported financially by the California Department of Transportation (Caltrans) through Agreement 65A0774 Amendment Number TO 005, and by the U.S. National Science Foundation (NSF) through Grant CMMI-1956248. Additional support was provided by the Faculty Chair in Earthquake Engineering Excellence at UC Berkeley. The findings, opinions, and conclusions presented in this paper are those of the authors and do not necessarily reflect the views of the sponsors. The views and conclusions contained in this document are also those of the authors and should not be interpreted as necessarily representing the official policies, either expressed or implied, of the U.S. Government or the State of California. Additionally, the NSF-sponsored Geotechnical Extreme Events Reconnaissance (GEER) Association funding through grant

CMMI-1266418 enabled researchers, including the second author, to document and learn from the case histories discussed in this report. The College of Engineering at the University of California, Berkeley (UCB), also provided support through the Faculty Chair in Earthquake Engineering Excellence.

The authors would also like to extend gratitude to the New Zealand government for openly sharing its CPT data and ground settlement data through the New Zealand Geotechnical Database (NZGD), as well as the engineers of Tonkin + Taylor, Ltd, and other engineers who provided data and managed the data collected following the New Zealand earthquakes. CentrePort, Wellington, is thanked for providing access to its site to document ground performance and characterize the ground, including assistance of Tiffany Palmer of the CentrePort Ltd.; Misko Cubrinovski, Ribu Dhakal, and Christopher de la Torre of the University of Canterbury; Emilia Stocks, Stuart Palmer, Mike Jacka, and Sjoerd van Ballegooy of Tonkin + Taylor; Iain Haycock of the McMillan Drilling Group; Hugh Cowan of the NZ EQC; and the aerial survey data from Cardno. We also thank ENGEO, Inc. for providing CPT data for Treasure Island, R. Luna for provided CPT data for the Treasure Island, J.P. Bardet for providing CPT data for the Marina District, and the U.S. Geologic Survey (USGS) and the New Generation Liquefaction (NGL) project for providing access to liquefaction reports and CPT data for Marina District and Treasure Island. We also thank all previous researchers who collected and shared data used in this research project. Additionally, discussions with Ribu Dhakal of the University of Canterbury about liquefaction effects in CentrePort are greatly appreciated.

ELECTRONIC SUPPLEMENTS

A *flatfile* summarizing the characteristics of the 205 case histories is the primary product of this study. It is shared as an electronic supplemental *Excel* file named *Supplemental_Free-field_Settl_case_histories_Flatfile_5SEP2022.xlsx*. In addition, the publicly available CPT data that support the case histories development and the details of each field case history are provided as electronic supplements.

REFERENCES

Abrahamson, C., Shi, M.H., and Yang, B. (2016). *Ground-Motion Prediction Equations for Arias Intensity Consistent with the NGA-West2 Ground-Motion Models*, PEER Report 2016/05, University of California, Berkeley, California.

Been, K. and Jefferies, M.G. (1985). "A State Parameter for Sands." *Geotechnique,* 35(2), 99-112.

Bennett, M.J. (1990). *Ground Deformation and Liquefaction of Soil in the Marina District. Effects of the Loma Prieta Earthquake on the Marina District San Francisco, California*, USGS Open-file Report, 90-253.

Bennett, M.J. (1998). *Sand Boils and Settlement on Treasure Island After the Earthquake. The Loma Prieta, California, Earthquake of October 17, 1989 – Liquefaction*, USGS Profesional Paper 1551-B.

Beyzaei, C.Z., Bray, J.D., van Ballegooy, S., Cubrinovski, M., and Bastin, S. (2018a). "Depositional Environment Effects on Observed Liquefaction Performance in Silt Swamps During the Canterbury Earthquake Sequence." *Soil Dyn. Earthq. Eng.,* 107, 303–321.

Beyzaei, C.Z., Bray, J.D., Cubrinovski, S., Riemer, M., and Stringer, M. (2018b). "Laboratory-based Characterization of Shallow Silty Soils in Southwest Christchurch." *Soil Dyn. Earthq. Eng.,* 110, 93-109.

Boulanger, R.W., and Idriss, I.M. (2014). *CPT and SPT Based Liquefaction Triggering Procedures*, Report No. UCD/CGM-14/01, University of California, Davis, CA.

Bradley, B.A. (2014). "Site-specific and Spatially-distributed Ground Motion Intensity Estimation in the 2010-2011 Christchurch Earthquakes." *Soil Dyn. Earthq. Eng.,* 48, 35–47

Bray, J.D. and Macedo, J. (2017). "6th Ishihara Lecture: Simplified Procedure for Estimating Liquefaction-induced Building Settlement." *Soil Dyn. Earthq. Eng*., 102, 215-231.

Bray, J.D. and Olaya, F.R. (2023). "2022 H. Bolton Seed Medal Lecture - Evaluating the Effects of Liquefaction." *J. Geotech Geoenviron Eng.*, 149(8).

Bray, J.D., Cubrinovski, M., Dhakal, R., and de la Torre, C. (2019). "Seismic Performance of CentrePort Wellington." *ASCE GeoCongress 2019 GSP 308*, 76 – 89.

Bray, J.D., Boulanger, R.W., Cubrinovski, M., Tokimatsu, K., Kramer, S.L., O'Rourke, T., Rathje, E., Green, R.A., Robertson, P., and Beyzaei, C.S. (2017). *U.S.–New Zealand–Japan International Workshop, Liquefaction-induced Ground Movements Effects, 2–4 November 2016*, PEER Report 2017/02, University of California, Berkeley, California.

Bullock, Z., Karimi, Z., Dashti, S., Porter, K., Liel, A.B., and Franke, K. W. (2019). "A physics-informed Semi-empirical Probabilistic Model for the Settlement of Shallow-founded Structures on Liquefiable Ground." *Geotechnique,* 69(5), 406 – 419.

California Department of Conservation. (2021). "CGS Map Sheet 48: Shear-wave Velocity in Upper 30m of Surficial Geology (Vs30)." <https://gis.data.ca.gov/datasets/cadoc::cgs-map-sheet-48-shear-wave-velocity-in-upper-30m-of-surficial-geology-vs30/about> (Sept. 2021).
Campbell, K.W., and Bozorgnia, Y. (2012). "A Comparison of Ground Motion Prediction Equations for Arias Intensity and Cumulative Absolute Velocity Developed Using a Consistent Database and Functional Form." *Earthq. Spectra*, 28, 931–941.
Cetin, K.O., Bilge, H.T., Wu, J., Kammerer, A.M., and Seed, R.B. (2009). "Probabilistic Models for Cyclic Straining of Saturated Clean Sands." *J. Geotech Geoenviron Eng,* 135(3), 71–86.
Chu, B.L., Hsu, S.C., and Chang, Y.M. (2003). "Ground Behavior and Liquefaction Analyses in Central Taiwan-Wufeng." *Engineering Geology*, 71, 119 -139.
Chu D. B., Stewart J.P., Lee S., Tsai J.S., Lin P.S., Chu B.L., Seed R.B., Hsu S.C., Yu M.S., Wang M. CH. (2004). Documentation of Soil Conditions at Liquefaction and Non-liquefaction Sites from 1999 Chi-Chi (Taiwan) Earthquake. *Soil Dyn. Earthq. Eng*., 24, 647 - 657, <https://rb.gy/s5mx7y> (Sept. 2021).
Cox, B.R., Boulanger, R.W., Tokimatsu, K., Wood, C.M., Abe, A., Ashford, S., and Donahue, J., et al. (2013). "Liquefaction at Strong Motion Stations and in Urayasu City During the 2011 Tohoku-Oki Earthquake." *Earthq. Spectra*, 29, S55 – S80.
Cubrinovski, M., Bray, J.D., de la Torre, C., Olsen, M., Bradley, B., Chiaro, G., Stocks, E., Wotherspoon, L., and Krall, T. (2018). "Liquefaction-Induced Damage and CPT Characterization of the Reclamations at CentrePort, Wellington." *Bull. Seismol. Soc. Am.,* 108, 1695 – 1708.
Cubrinovski, M., and Ishihara, K. (2002). "Maximum and minimum void ratio characteristics of sands." *Soils Found*., 42(6), 65–78.
Cubrinovski, M., Rhodes, A., Ntritsos, N., and van Ballegooy, S. (2019). "System response of liquefiable deposits." *Soil Dyn. Earthq. Eng*., 124(1), 212–29.
Deierlein, G., Krawinkler, H., and Cornell, C., (2003). "A Framework for Performance-based Earthquake Engineering." *Pacific Conference on Earthquake Engineering*, Christchurch, New Zealand.
Dhakal, R., Cubrinovski, M., and Bray, J. D. (2020). "Geotechnical Characterization and Liquefaction Evaluation of Gravelly Reclamations and Hydraulic Fills (port of Wellington, New Zealand)." *Soils Found.,* 60(6),1507–31.
Dhakal, R., Cubrinovski, M., and Bray, J.D. (2022). "Evaluating the Applicability of Conventional CPT-based Liquefaction Assessment Procedures to Reclaimed Gravelly Soils." *Soil Dyn. Earthq. Eng*., 155, 107176.
ENGEO (2015). *Geotechnical Data Report (GDR)*, Sub-Phase 1A, Treasure Island, San Francisco, California, Project No 7091.000.000.
ENGEO (2019a). *Geotechnical Exploration,* Wastewater Treatment Plant, Treasure Island, San Francisco, Project No. 7091.000.005.
ENGEO (2019b). *Geotechnical Characterization Report*, Treasure Island Stages 2 and 3 Major Phase 1, Subphases 1A, 1D, 1F, 1G, 1H, 1I Infrastructure Improvements, San Francisco, California, Project No. 7091.000.003.
ENGEO (2019c). *Geotechnical Design Report*, Treasure Island Stages 2 and 3 Major Phase 1, Subphases 1A, 1D, 1F, 1G, 1H, 1I Infrastructure Improvements, San Francisco, California, Project No. 091.000.003, DRAFT.
Foulser-Piggott, R., and K. Goda (2015). "Ground-motion Prediction Models for Arias Intensity and Cumulative Absolute Velocity for Japanese Earthquakes Considering Single-station Sigma and Within Event Spatial Correlation." *Bull. Seismol. Soc. Am*., 105(4), 1903–1908.
Geyin, M., and Maurer, B. (2020). "Fragility Functions for Liquefaction-Induced Ground Failure." *J. Geotech Geoenviron Eng,* 146(12), 04020142.
Gregor, N., Abrahamson, N.A., Atkinson, G.M., Boore, D.M., Bozorgnia, Y., Campbell, K.W., Chiou, B.S.J., Idriss, I.M., Kamai, R., Seyhan, E. and Silva, W. (2014). "Comparison of NGA-West2 GMPEs." *Earthquake Spectra*, 30(3),1179-1197.
Holzer, T. L., Noce, T.E., and Bennett., M.J. (2010). *Maps and documentation of seismic CPT soundings in the central, eastern, and western United States*: U.S. Geological Survey Open-File Report 2010-1136.
Hryciw, R. D. (1991). *Post Loma Prieta Earthquake CPT, DMT and Shear Wave Velocity Investigations of Liquefaction Sites in Santa Cruz and on Treasure Island*, Final Report to the USGS Award No. 14-08-0001-G1865.
Hutabarat, D., and Bray J.D. (2021). "Seismic Response Characteristics of Liquefiable Sites with and without Sediment Ejecta Manifestation." *J. Geotech Geoenviron Eng*., 147(6), 10.1061/(ASCE)GT.1943-5606.0002506.
Hutabarat, D., and Bray, J.D. (2022). "Estimating the Severity of Liquefaction Ejecta Using the Cone Penetration Test." *J. Geotech Geoenviron Eng.* 148(3), 10.1061/(ASCE)GT.1943-5606.0002744.
Idriss, I., and Boulanger, R. (2008). *Soil Liquefaction During Earthquakes*, Earthquake Engineering Research Institute (EERI), MNO-12.

Ishihara, K., and Yoshimine, M. (1992). "Evaluation of Settlements in Sand Deposits Following Liquefaction During Earthquakes." *Soils Found*., 32(1),173–188.
Juang, C.H. (2002). "Investigation of Soil Liquefaction in the 1999 Chi-Chi, Taiwan, Earthquake." *National Science Foundation, CMMI-0085143*, < http://hsein.people.clemson.edu/> (Sept. 2021).
Juang, C.H., Yuan, H., Lee, D.H., and Ku, C-S. (2002). "Assessing CPT-based Methods for Liquefaction Evaluation with Emphasis on the Cases from the Chi-Chi, Taiwan, Earthquake." *Soil Dyn. Earthq. Eng.,* 22, 241–258.
Juang, C., Ching, J., Wang, L., Khoshnevisan, S., and Ku, C-S. (2013). "Simplified Procedure for Estimation of Liquefaction-induced Settlement and Site-specific Probabilistic Settlement Exceedance Curve Using Cone Penetration Test (CPT)." *Can Geotech J*., 50(10), 2013.
Katsumata, K., and Tokimatsu, K. (2012). "Relationship Between Seismic Characteristics and Liquefaction Damages of Urayasu City Induced by the 2011 Great East Japan Earthquake." *9th International Conference on Urban Earthquake Engineering/ 4th Asia Conference on Earthquake Engineering.*
Kayen, R.E., and Mitchell, J.K. (1997). "Arias Intensity Assessment of Liquefaction Test Sites on the East Side of San Francisco Bay Affected by the Loma Prieta, California, Earthquake of 17 October 1989." *Natural Hazards,* 16: 243–265, 1997.
Kokusho, T., Nagao, Y., Ito, F., and Fukuyama, T. (2014). "Sand Liquefaction Observed During Recent Earthquake and Basic Laboratory Studies on Aging Effect." *Earthquake Geotechnical Engineering Design 28*.
Ku, C.S., Juang, C. H., Chang, C. W., and Ching, J. (2012). "Probabilistic Version of the Robertson and Wride Method for Liquefaction Evaluation: Development and Application." *Canadian Geotechnical J.*, 49(1), 27-44.
Lee, K. L., and Albaisa, A. (1974). "Earthquake Induced Settlements in Saturated Sands." *J. Geotech. Eng. Division*, GT4, 387-406.
Lee, W.F., Ishihara, K., Chen, S.H., and Chu, B.L. (2011). "Liquefaction Induced Ground Failures Caused by Strong Ground Motion." *5th international Conference on Earthquake Geotechnical Engineering*, Paper No. ASOLE.
Liu, K.S., and Tsai, Y.B. (2015). "A Refined Vs30 Map for Taiwan Based on Ground Motion Attenuation Relationships." *Terrestrial, Atmospheric and Oceanic Sciences Journal,* 26(6).
Macedo, J., Abrahamson, N., and Bray, J.D. (2019). "Arias Intensity Conditional Scaling Ground-Motion Models for Subduction Zones." *Bull. Seismol. Soc. Am*., 109(4), 1343 – 1357.
Macedo, J., Abrahamson, N., and Liu, C. (2021). "New Scenario-Based Cumulative Absolute Velocity Models for Shallow Crustal Tectonic Settings." *Bull. Seismol. Soc. Am*., 111(4), 157 – 172.
Markham, C.S., Bray, J.D., Macedo, J., and Luque R. (2016). "Evaluating Nonlinear Effective Stress Site Response Analyses Using Records from the Canterbury Earthquake Sequence." *Soil Dyn. Earthq. Eng.,* 82, 84–98.
Maurer, B.W., Green, R.A., van Ballegoy, S., and Wotherspoon, L. (2019a). "Development of Region-specific Soil Behavior Type Index Correlations for Evaluating Liquefaction Hazard in Christchurch, New Zealand." *Soil Dyn. Earthq. Eng.,* 117, 96–105.
Maurer, B.W., Green, R.A., Cubrinovski, M., and Bradley, B.A. (2019b). "Evaluation of the Liquefaction Potential Index for Assessing Liquefaction Hazard in Christchurch, New Zealand." *J. Geotech Geoenviron Eng.,* 140, 04014032-1.
Mesri, G., Shahien, M., and Kane, T. (2018). "Seismically Induced Settlement of Ground Experiencing Undrained Shaking and Laterally Constrained Compression." *Can Geotech J.*, 1-18.
Mijic, Z., Bray, J.D., and van Ballegoy, S. (2021). *Detailed Evaluation of Insightful Liquefaction Ejecta Case Histories for the Canterbury Earthquake Sequence, New Zealand*, USGS G20AP00079 Technical Report.
Mitchell, J. and Soga, K. (2005). *Fundamentals of soil behavior*, 3rd edition, John Wiley & Sons, Hoboken.
McGann, C.R., Bradley, B.A., and Cubrinovski, M. (2017). "Development of a Regional Vs30 Model and Typical Vs Profiles for Christchurch, New Zealand from CPT Data and Region-specific CPT-Vs correlation." *Soil Dyn. Earthq. Eng*., 95.
National Research Council (NRC) (2016). *State of the Art and Practice in the Assessment of Earthquake Induced Soil Liquefaction and Its Consequences*, Committee on Earthquake Induced Soil Liquefaction Assessment, DC: The National Academies Press, Washington.
New Zealand Geotechnical Database (NZGD) (2021). "New Zealand Geotechnical Database." *New Zealand Earthquake Commission*, <https://www.nzgd.org.nz/> (Sept. 2021).
O'Rourke, T.D., and Roth, B.L. (1990). *Performance of Pipeline Systems in the Marina. Effects of the Loma Prieta Earthquake on the Marina District San Francisco, California*, USGS Open-file Report 90-253.
Olaya, F.R., and Bray, J.D. (2022). "Strain Potential of Liquefied Soil." *J. Geotech Geoenviron Eng*., ASCE, in press.
Power, M.S., Egan, J.A., Shewbridge, S.E., deBecker, J., and Faris R. (1998). *Analysis of Liquefaction-induced Damage on Treasure Island. The Loma Prieta, California, Earthquake of October 17, 1989 – Liquefaction*, USGS Professional Paper 1551-B.
Robertson, P.K. (2009a). "Interpretation of Cone Penetration Tests – A Unified Approach." *Can. Geotech J.*, 46(11), 1337–1355.

Robertson, P.K. (2009b). "Performance-based Earthquake Design Using the CPT." *International Conference on Performance-Based Design in Earthquake Geotechnical Engineering,* (Is-Tokyo 2009).
Robertson, P.K. (2010). "Estimating In-situ State Parameter and Friction Angle in Sandy Soils from CPT." *2nd International Symposium on cone Penetration Testing*.
Robertson, P.K., and Cabal K.L. (2015). *Guide to CPT for Geotechnical Engineering*, 6th ed., Gregg Drilling Testing, Inc. Signal Hill, CA.
Robertson, P.K., and Wride, C.E. (1998). "Evaluating Cyclic Liquefaction Potential Using the Cone Penetration Test." *Can. Geotech. J*., 35(3), 442–459.
Russell, J., and van Ballegooy, S. (2015). *Canterbury Earthquake Sequence: Increased Liquefaction Vulnerability Assessment Methodology*, T+T Report 0028-1-R-JICR-2015 prepared for the Earthquake Commission.
Sadeghi, H., Pak, A., Pakzad, A., and Ayoubi, P. (2021). "Numerical-probabilistic Modeling of the Liquefaction-induced Free Fields Settlement." *Soil Dyn. Earthq. Eng.,* 149, 106868.
Tokimatsu, K., and Seed, H.B. (1977). "Evaluation of Settlement in Sands due to Earthquake Shaking." *J.Geotech. Eng. Division*, 113(8), 861-878.
Tokimatsu, K., and Katsumata, K. (2012). "Liquefaction-induced Damage to Buildings in Urayasu City During the 2011 Tohoku Pacific Earthquake." *International Symposium on Engineering Lessons Learned from the 2011 Great East Japan Earthquake.*
USGS (2021a). "United States Geological Survey - Map of CPT Data." <https://earthquake.usgs.gov/research/cpt/data/> (Sept. 2021).
USGS (2021b). "United States Geological Service Vs30 Models Marina District and Treasure Island sites, <https://earthquake.usgs.gov/data/vs30/> (Sept. 2021).
Vantassel, J., Cox, B., Wotherspoon, L., and Stolte, A., (2018). "Mapping Depth to Bedrock, Shear Stiffness, and Fundamental Site Period at CentrePort, Wellington, Using Surface-Wave Methods: Implications for Local Seismic Site Amplification." *Bull. Seismol. Soc. Am.,* 108(38).
Wu, J., and Seed, R. B. (2004). "Estimating of Liquefaction-induced Ground Settlement Case Studies." *Proc., 5th Int. Conf. on Case Histories in Geotechnical Engineering*, Paper 3.09.
Yasuda, S., Ishihara, K., Harada, K., and Shinkawa, N. (1996). "Effect of Soil Improvement on Ground Subsidence due to Liquefaction." *Soils Found.*, Special Issue, 99-107.
Yoshimine, M., Nishizaki, H., Amano, K., and Hosono, Y. (2006). "Flow Deformation of Liquefied Sand Under Constant Shear Load and its Applications to Analysis of Flow Slide in Infinite Slope." *Soil Dyn. Earthq. Eng.,* 26, 253–264.
Zhang, G., Robertson, P.K., and Brachman, R.W.I. (2002). "Estimating Liquefaction-induced Ground Settlements from CPT for Level Ground." *Can. Geotech J.*, 39, 1168–1180.
Zimmaro, P., Brandenberg, S.J., Stewart, J.P., Kwak, D.Y., Franke, K.W., Moss, R.E.S., Cetin, K.O., Can, G., Ilgac, M., Stamatakos, J., Juckett, M., Mukherjee, J., Murphy, Z., Ybarra, S., Weaver, T., Bozorgnia, Y., and Kramer, S.L. (2019). "Next-Generation Liquefaction Database." Next-Generation Liquefaction Consortium <https://www.nextgenerationliquefaction.org/> (Sept 2021).

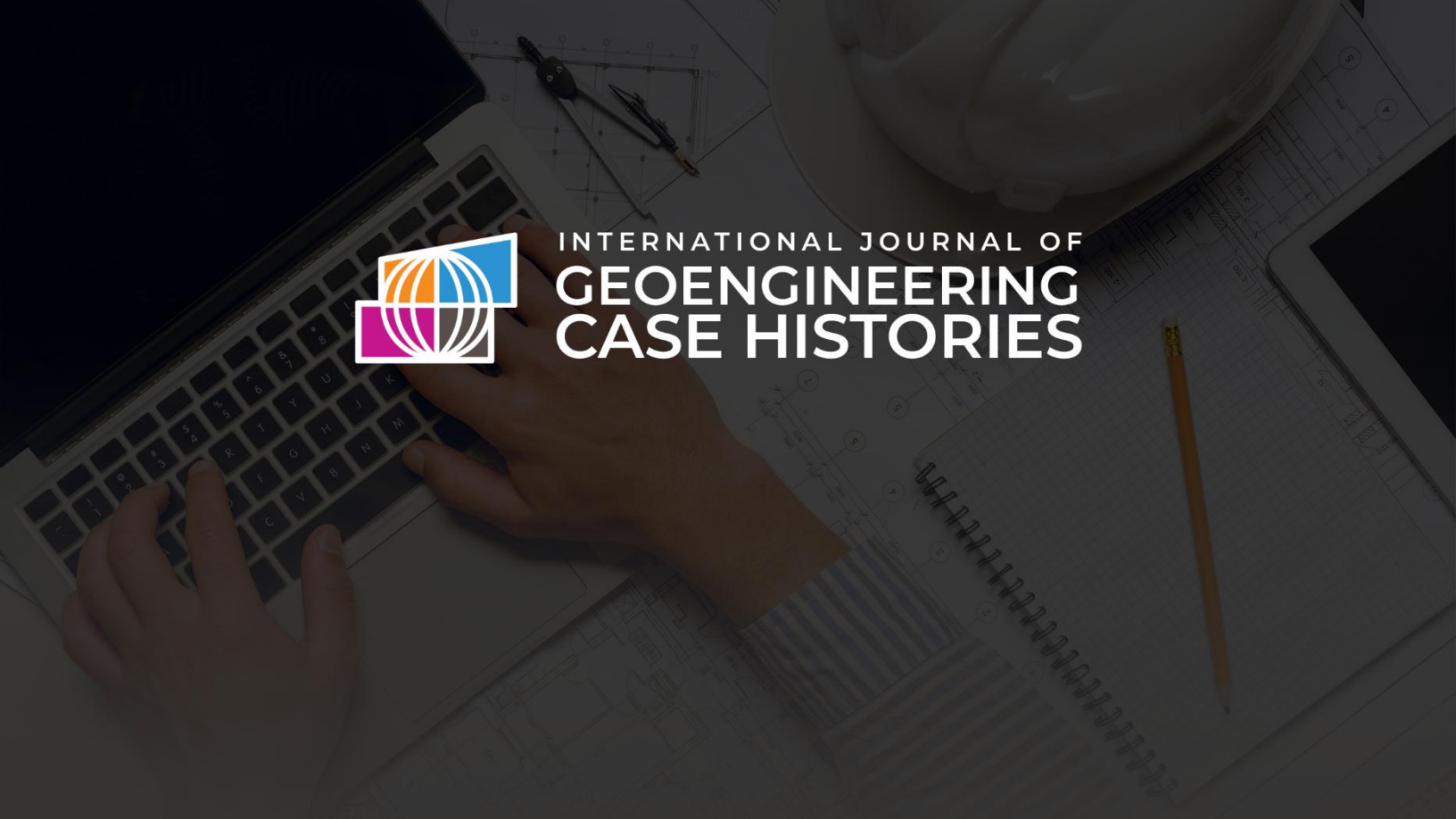

INTERNATIONAL JOURNAL OF
GEOENGINEERING
CASE HISTORIES

The Journal's Open Access Mission is generously supported by the following Organizations:

dar
a Sidara company

Geosyntec consultants
engineers | scientists | innovators

CONETEC
MUD BAY DRILLING
LANKELMA
Geotech DRILLING

ENGEO
Expect Excellence

Access the content of the ĪSSMGE Īnternational Journal of Geoengineering Case Histories at:
www.geocasehistoriesjournal.org

Downloaded: Tuesday, October 06 2026, 00:26:02 UTC